BIOCHEMISTRY
including biophysical chemistry & molecular biology

Article

pubs.acs.org/biochemistry

Structure of the Apo Form of *Bacillus stearothermophilus* Phosphofructokinase

Rockann Mosser, Manchi C. M. Reddy, John B. Bruning, James C. Sacchettini, and Gregory D. Reinhart*

Department of Biochemistry and Biophysics, Texas A&M University and Texas AgriLife Research, College Station, Texas 77843-2128, United States

ABSTRACT: The crystal structure of the unliganded form of *Bacillus stearothermophilus* phosphofructokinase (BsPFK) was determined using molecular replacement to 2.8 Å resolution (Protein Data Bank entry 3U39). The apo BsPFK structure serves as the basis for the interpretation of any structural changes seen in the binary or ternary complexes. When the apo BsPFK structure is compared with the previously published liganded structures of BsPFK, the structural impact that the binding of the ligands produces is revealed. This comparison shows that the apo form of BsPFK resembles the substrate-bound form of BsPFK, a finding that differs from previous predictions.

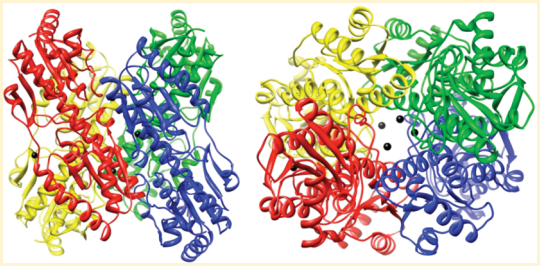

Phosphofructokinase (PFK) is under strong metabolic regulation because it catalyzes the first committed step of glycolysis in which it transfers the γ-phosphate from MgATP to fructose 6-phosphate (Fru-6-P), yielding MgADP and fructose 1,6-bisphosphate (F1,6BP). Not surprisingly, PFK is the subject of intense study and often serves as a key example of an allosteric enzyme.[1,2] Eukaryotic PFKs have a very complex regulation involving many effectors.[3] Recently, the structures of PFK from baker's yeast and rabbit muscle have been determined.[3−7] Insight into the allosteric regulation of eukaryotic PFKs can be gleaned by the study of the much simpler regulation exhibited by prokaryotic PFKs. The two most thoroughly characterized type 1 prokaryotic PFKs are from *Escherichia coli* (Ec) and *Bacillus stearothermophilus* (Bs)[4,5] (a second, nonhomologous type 2 PFK also exists in bacteria[36]). EcPFK and BsPFK have 55% identical amino acid sequences, and both are homotetramers with a molecular mass of 34 kDa per subunit.[6] Both enzymes are regulated by the K-type effectors (allosteric ligands that alter the binding of the substrate) phosphoenolpyruvate (PEP), an allosteric inhibitor, and MgADP, an allosteric activator. Furthermore, PEP and MgADP bind to the same allosteric site. EcPFK and BsPFK have two unique dimer−dimer interfaces: the substrate-binding interface and the effector-binding interface. The substrate-binding interface contains the Fru-6-P binding site, which is comprised of amino acids from two adjacent subunits. Likewise, the effector-binding interface possesses the allosteric ligand binding site that consists of amino acids from two adjacent subunits. Each homotetramer possesses four identical Fru-6-P binding sites and four identical effector binding sites.

Currently, there are seven crystal structures of bacterial ATP-dependent type 1 PFKs in the Protein Data Bank (PDB). Of the seven structures, only one does not originate from EcPFK or BsPFK. *Lactobacillus delbrueckii* PFK (LbPFK) is 56 and 47% identical in amino acid sequence to BsPFK and EcPFK, respectively.[7] Despite the high degree of sequence identity LbPFK shares with EcPFK and BsPFK, LbPFK exhibits a severely diminished capacity to bind both PEP and MgADP.[8] The structure of LbPFK with SO_4 bound to all four active sites and all four effector sites (PDB entry 1ZXX) was determined by Paricharttanakul et al.[8] The crystal structures of EcPFK include the apo enzyme, which was grown in the absence of ligands (PDB entry 2PFK),[9] and the enzyme bound to its reaction products (PDB entry 1PFK).[10] The latter structure contains the bound reaction products F1,6BP and MgADP in all four active sites, and MgADP is bound to all four effector binding sites. Comparison of the two EcPFK crystal structures to each other reveals that their secondary, tertiary, and quaternary structures are nearly identical.

Each of the three crystal structures of BsPFK contains different combinations of bound ligands. Evans et al. crystallized BsPFK in a solution containing Fru-6-P and then washed the crystal with a phosphate solution. The phosphate solution reportedly displaced any Fru-6-P bound and allowed the structure of the phosphate-bound BsPFK (PDB entry 3PFK)[11]to be determined. The phosphate-bound form of BsPFK contains a phosphate molecule at each of the Fru-6-P and effector binding sites for a total of eight bound phosphate moieties. The crystal structure of BsPFK bound to Fru-6-P and MgADP in all substrate binding sites and MgADP in all of the effector binding sites (PDB entry 4PFK)[12] was determined by Evans et al. and will be termed the "substrate-bound" BsPFK in the following discussion. BsPFK was also crystallized in the presence of phosphoglycolate (PGA), an analogue of the inhibitor PEP, and the structure reveals that PGA is bound to all four effector binding sites (PDB entry 6PFK).[13] In a study comparing the binding affinities and allosteric properties of BsPFK with PGA and PEP, it was found that PGA inhibits

Received: October 6, 2011
Revised: December 30, 2011
Published: January 2, 2012

BsPFK in a manner similar, though not identical, to that of PEP.[14] The structures of the phosphate-bound enzymes and substrate-bound enzymes are very similar to each other; however, the PGA-bound BsPFK displays a different conformation.

The crystal structure of BsPFK containing the W179F and Y164W modifications revealed that Fru-6-P and MgADP were bound in all substrate-binding sites and MgADP occupied all four effector binding sites (PDB entry 1MTO).[15] This structure was also found to resemble the substrate-bound form of BsPFK. This variant of BsPFK apparently dissociates in the presence of PEP.[15]

Before any crystal structures of PFK had been determined, the allosteric behavior of EcPFK was described using the concerted transition model proposed by Monod, Wyman, and Changeux (MWC).[5,16] Upon determining the structures of the substrate-bound forms and PGA-bound forms of BsPFK, Schirmer and Evans interpreted the differences in these structures in terms of the MWC model.[13] The enzyme was described as existing in two states, the substrate-bound form (R-state) and the PGA-bound form (T-state). Comparison of the substrate-bound and PGA-bound structures of BsPFK reveals that the PGA-bound form has undergone a 7° rotation about the substrate-binding interface, termed the quaternary shift. This shift is accompanied by secondary and tertiary changes that include the unwinding of the end of helix 6 and the displacement of Arg 162 with Glu 161 in the Fru-6-P binding site. Evans et al. did not obtain an apo BsPFK structure but concluded that the structure must assume the T-state conformation because crystals cracked when substrate was removed.[11,12] This prediction was a direct result of assuming the enzyme exists in only two states.

In this paper, we present the crystal structure of the apo form of wild-type BsPFK, determined to 2.8 Å resolution. This crystal structure serves as a basis for comparison of any structural changes seen in the binary or ternary complexes, and thus, it is particularly significant. In addition, the tertiary and quaternary structures of apo BsPFK are different from those originally predicted by Evans et al.[11,12] Contrary to prior expectations, the apo form of BsPFK resembles the substrate-bound form of the enzyme more than it does the PGA-bound form. The structure of the apo form of BsPFK is therefore an important addition to the structural library of allosterically relevant enzyme forms that will help us better understand the structural basis of the allosteric mechanism.

MATERIALS AND METHODS

Materials. All chemical reagents used in buffers, protein purifications, and enzymatic assays were of analytical grade, purchased from Sigma-Aldrich (St. Louis, MO) or Fisher Scientific (Fair Lawn, NJ). Creatine kinase and the ammonium sulfate suspension of glycerol-3-phosphate dehydrogenase were purchased from Roche (Indianapolis, IN). The ammonium sulfate suspensions of aldolase and triosephosphate isomerase and the sodium salts of phosphocreatine, ATP, and phosphoenolpyruvate were purchased from Sigma-Aldrich. The coupling enzymes, obtained as ammonium sulfate suspensions, were extensively dialyzed against MOPS buffer [50 mM MOPS-KOH (pH 7.0), 100 mM KCl, 5 mM $MgCl_2$, and 0.1 mM EDTA] before being used. The sodium salt of Fru-6-P was purchased from Sigma-Aldrich or USB Corp. (Cleveland, OH). NADH and DTT were purchased from Research Products International (Mt. Prospect, IL), and the crystallization reagents were purchased from Hampton Research (Aliso Viejo, CA). Mimetic Blue 1 resin used for protein purification was purchased from Prometic Biosciences (Rockville, MD). Deionized distilled water was used throughout.

Protein Purification. Plasmid pBR322/BsPFK[17] contains the gene for BsPFK behind the native *B. stearothermophilus* promoter and was received as a generous gift from Simon H. Chang (Louisiana State University, Baton Rouge, LA). Wild-type BsPFK was expressed in *E.coli* RL257 cells,[18] which is a strain of *E. coli* lacking both the *pfkA* and *pfkB* genes. The purification of BsPFK was performed as described previously, with a few modifications.[19] RL257 cells containing plasmid pBR322/BsPFK were grown at 37 °C for 16−18 h in LB (Luria-Bertani) broth/ampicillin (10 g/L Tryptone, 5 g/L yeast extract, and 10 g/L sodium chloride with 100 μg/mL ampicillin). Cells were centrifuged and frozen at −20 °C for at least 12 h. The cells were resuspended in purification buffer [10 mM Tris-HCl and 1 mM EDTA (pH 8.0)] and sonicated in a Fisher 550 Sonic Dismembrator at 0 °C via 15 s pulses at setting 6 for 8 min. The crude lysate was centrifuged using a Beckman model J2-21 centrifuge at 22500*g* for 1 h at 4 °C. The clear supernatant was heated at 70 °C for 15 min, cooled on ice for 15 min, and centrifuged for 1 h at 4 °C. The supernatant was diluted 4-fold and then loaded onto a Mimetic Blue 1 column that was equilibrated with purification buffer. The column was washed with at least 5 bed volumes of purification buffer, and the enzyme was eluted with a 0 to 1 M NaCl gradient. Fractions containing enzyme were pooled and dialyzed into 20 mM Tris-HCl (pH 8.5) and loaded onto a Pharmacia Mono-Q anion exchange column. The enzyme was eluted with a 0 to 1 M NaCl gradient, and fractions containing PFK were combined, concentrated, and then dialyzed into EPPS buffer [50 mM EPPS, 10 mM $MgCl_2$, 100 mM KCl, and 0.1 mM EDTA (pH 8.0)]. The concentrated enzyme was stored in EPPS buffer at 4 °C. The final enzyme was determined to be pure by sodium dodecyl sulfate−polyacrylamide gel electrophoresis, and the concentration was ascertained using the absorbance at 280 nm (ε = 18910 M^{-1} cm^{-1}[20]).

Crystallization and Data Collection. BsPFK was crystallized using the hanging drop vapor diffusion method[21] at 16 °C. Crystallization was achieved in a 4 μL drop consisting of 1 μL of well solution [0.2 M calcium acetate hydrate, 0.1 M sodium cacodylate trihydrate (pH 6.5), and 18% (w/v) polyethylene glycol 8000] and 3 μL of protein (the stock concentration of BsPFK was 28 mg/mL). Within 24 h, BsPFK crystals of a plate morphology were formed. The crystals were briefly soaked in well solution with 30% ethylene glycol and then flash-cooled in a liquid N_2 stream at 100 K. Diffraction data were collected on Advanced Photon Source beamline 23-ID using a MAR 300 CCD detector (MarMosaic from Marresearch-Charged Coupled Device) (Rayonix LLC, Evanston, IL). The HKL2000 program package (HKL Research, Inc., Charlottesville, VA)[22] was used for integration and scaling.

Structure Determination and Refinement. The molecular replacement program PHASER (University of Cambridge, Cambridge, U.K.)[23] was used to determine the structure of apo BsPFK using the phosphate-bound crystal structure of BsPFK (PDB entry 3PFK)[12] with waters and ions removed as a search model. Rigid body refinement followed by simulated annealing refinement at 5000 K was conducted using Phenix (Python-based Hierarchical Environment for Integrated Xtallography).[24]

Subsequently, refinement was conducted in alternating cycles of manual model building in COOT (Crystallographic Object-Orientated Toolkit)[25] followed by refinement in Phenix until the *R* factors converged. The stereochemical quality of the final model of the apo BsPFK enzyme was verified with MolProbity (Duke University, Durham, NC).[26] The coordinates have been deposited in the PDB as entry 3U39. Molecular graphics images were produced using the UCSF Chimera package from the Resource for Biocomputing, Visualization, and Informatics at the University of California, San Francisco, CA (supported by National Institutes of Health Grant P41 RR-01081).[27]

RESULTS

Apo BsPFK crystals belong to space group *C*2 with the unit cell dimensions listed in Table 1. Figure 1 shows the asymmetric unit that consists of four subunits or a single tetramer with an estimated solvent content of 58.5%. The final structure has a 2.8 Å resolution. The entire structure consists of 1276 residues (319 residues per monomer), 326 water molecules, and five calcium ions. The details of the final data processing and refinement parameters are listed in Table 1.

Table 1. Data Collection and Refinement Statistics for Apo BsPFK[a]

unit cell (Å)	a = 202
	b = 113
	c = 77
	β = 104
space group	*C*2
no. of molecules per asymmetric unit (*Z*)	four subunits
resolution (Å)	50−2.8
completeness (%)	98.8 (99.2)
I/I	14.61 (2.80)
R_{sym}	11.5 (46.0)
refinement	
resolution (Å)	50−2.8
no. of reflections (working/free)	38382 (1933)
R (%)	19.90
R_{free} (%)	26.01
no. of protein atoms/no. of waters	9384/326
average *B* factor (Å^2)	42.91
average *B* factor for water molecules (Å^2)	44.83
rmsd for bond lengths (Å)	0.004
rmsd for bond angles (deg)	0.620
Ramachandran statistics (%)	
most favored	95.82
allowed	3.63

[a]For details of the crystallization and structure determination, see the text. Values in parentheses are for high-resolution shells. $R_{sym} = \sum_h\sum_i |I_{hi} - \langle I_h\rangle|/\sum_h\sum_i I_{hi}$, where I_{hi} is the *i*th observation of reflection *h*, whereas $\langle I_h\rangle$ is the mean intensity of reflection *h*. $R_{cryst} = \sum||F_o| - |F_c||/|F_o|$. R_{free} was calculated with a fraction (5%) of randomly selected reflections excluded from refinement. rmsd, root-mean-square deviation from ideal geometry.

The five calcium ions are most likely a crystallization artifact because calcium is a main component of the crystallization solution. Figure 1 shows the calcium ions and how they appear to bind to the enzyme randomly. Four of the ions associate with aspartate residues, and the fifth ion associates with two water molecules and possibly a backbone carbonyl group. Each Asp 155 from subunits A−C is associated with a calcium ion, and Asp 307 from subunit D is associated with the fourth ion. Neither Asp 155 nor Asp 307 is involved in the direct binding of any ligand, and the ions are asymmetrically located in the structure. In addition, there are no experimental data to suggest that calcium affects either the ligand binding or the allosteric nature of BsPFK. Apart from the nonspecifically bound calcium ions, there are no other ligands bound to the enzyme.

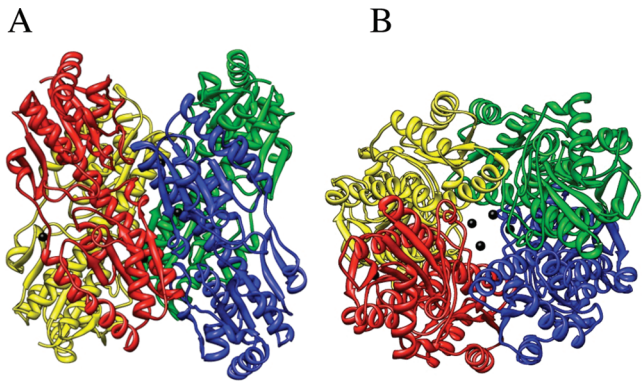

Figure 1. Apo BsPFK tetramer, with subunit A colored blue, subunit B colored green, subunit C colored yellow, subunit D colored red, and calcium ions colored black. (A) View of apo BsPFK showing the substrate-binding interface between red and blue monomers and green and yellow monomers and the allosteric interface between red and yellow monomers and blue and green monomers. (B) Alternate view, rotated 90° along the horizontal axis.

The root-mean-square deviation (rmsd) between apo BsPFK and the substrate-bound BsPFK is 0.53 ± 0.05 Å for 319 Cα atoms. The rmsd between apo BsPFK and the PGA-bound BsPFK is 0.94 ± 0.05 Å for 319 Cα atoms. The quaternary structures of the apo, substrate-bound, and PGA-bound forms were compared using the structure comparison tools of UCSF Chimera.[27] Because the substrate-bound PDB file produces a single subunit in the asymmetric unit, the tetramer was generated with the unit cell function of Chimera by use of the crystallographic symmetry operators. Using the match-maker function of Chimera, the apo structure was designated the reference structure with which the other two structures would be compared. One subunit in the apo structure aligned with one subunit in the substrate-bound and PGA-bound forms. Once the alignment was completed, each subunit was represented with a different color, which allowed the substrate-binding and effector-binding interfaces to be distinguished.

To determine the rotation about the substrate-binding interface introduced by the binding of ligand, as first described by Schirmer and Evans,[13] the angle of the plane of the effector-binding interface was measured. Schirmer and Evans reported a 7° rotation about the substrate-binding interface when they compared the substrate-bound and PGA-bound forms of BsPFK;[13] however, using the method just described, we observed an 8° rotation. The 1° difference is most likely due to the different techniques used in determining the angles. The angle we measured for the substrate-bound BsPFK structure is −1° when compared to the apo structure, and the angle measured for the PGA-bound structure is 7° when compared to the apo structure. Therefore, the quaternary structure of apo BsPFK is similar, but not identical, to the quaternary structure of substrate-bound BsPFK (Figure 2). Given the values for the rmsds and the state of the quaternary structures, it appears that the apo enzyme is more like the substrate-bound form than the

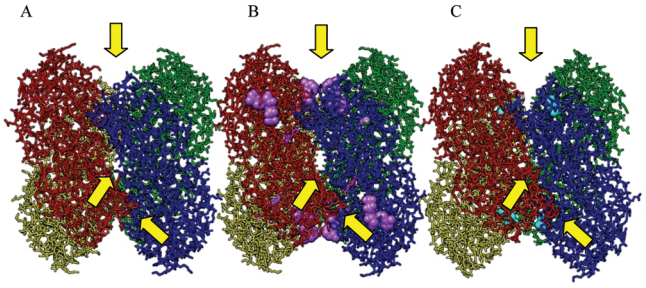

Figure 2. Comparison of wild-type BsPFK crystal structures. (A) Apo BsPFK. (B) Substrate-bound BsPFK (PDN entry 4PFK)[12] with active site and effector site ADP in space filling form (purple). (C) PGA-bound BsPFK (PDB entry 6PFK)[13] with PEP in space filling form (cyan). The blue monomer was aligned to the blue monomer of the apo structure for each ligand-bound structure. Each monomer is colored blue, green, yellow, and red. The substrate-binding interfaces are between the red and blue monomers and between the green and yellow monomers. The effector-binding interfaces are between the green and blue monomers and between the red and yellow monomers. Areas where there are differences in the tertiary and quaternary structures are denoted with yellow arrows.

PGA-bound form. By contrast, Evans et al.[11,12] observed that when crystals formed in the presence of Fru-6-P were transferred to a solution lacking any activating ligands, the crystals cracked. Also, crystals grown in the presence of an inhibitor cracked when exposed to Fru-6-P. The cracking of the crystals was interpreted as being an indicator of the enzyme undergoing a large conformational shift, presumably the quaternary shift. However, it is clear that the enzyme has not undergone the quaternary shift to the same extent as seen in the PGA-bound structure when crystallized only in the presence of the crystallization solvent. One should note, however, that there are also many local differences observed among the apo, substrate-bound, and PGA-bound structures.

Figure 3 shows the electron density map of the residues comprising the Fru-6-P binding site and the effector binding site. Some of the Lys and Arg side chains were omitted because of missing or ambiguous density, likely due to their positions being mobile in the absence of interaction with the missing ligand. The mean positional error of the atoms of the entire structure was calculated by a Luzzati plot to be 0.35 Å.[40]

Figure 4 compares the Fru-6-P binding site of apo BsPFK to the substrate-bound and the PGA-bound forms of BsPFK. Overall, the orientations of the residues in the active site for the

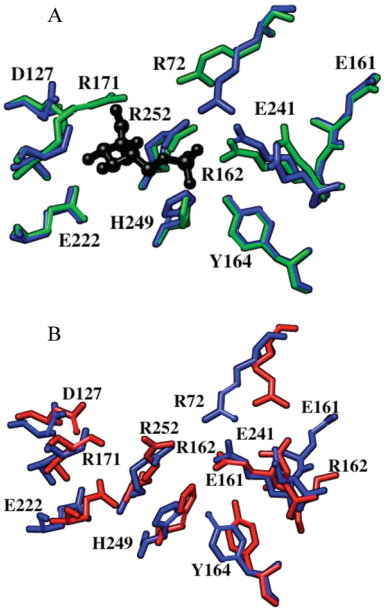

Figure 4. Overlay of residues in the Fru-6-P binding site of BsPFK. (A) Apo residues colored blue, substrate-bound BsPFK residues colored green, and Fru-6-P shown as black balls and sticks. (B) Apo residues colored blue and PGA-bound BsPFK residues red. All residues are labeled.

apo structure appear to correspond better with the active site residues of substrate-bound BsPFK than those of PGA-bound BsPFK. However, there are a few key residues with changes in orientation that have altered interactions that could not have been predicted without the apo BsPFK crystal structure. For instance, Arg 72 interacts with the phosphate groups of ATP in the substrate-bound enzyme. In the PGA-bound BsPFK where ATP is no longer bound, Arg 72 forms a salt bridge with Glu 241 across the substrate-binding interface. The orientation of Arg 72 in apo BsPFK is different from those of both liganded forms of BsPFK. In apo BsPFK, Arg 72 does not form a salt bridge with Glu 241.

His 249 is another residue that exhibits a difference in its orientation in the apo structure as compared to either liganded structure. In the substrate-bound enzyme, His 249 interacts with the phosphate group of Fru-6-P. His 249 forms a hydrogen bond across the substrate-binding interface with Glu 161 in the PGA-bound structure. In the apo structure, His 249

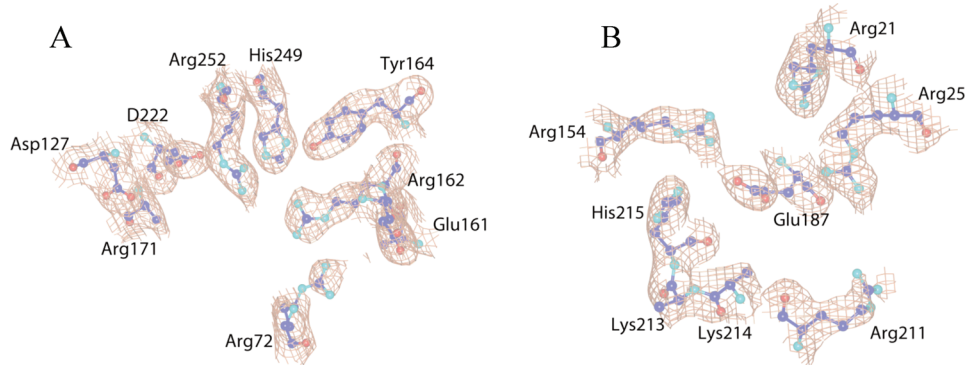

Figure 3. Electron density of the apo PFK Fru-6-P binding site (A) and effector site (B). Figures were rendered in CCPRMG molecular graphics software.[38] Shown in coral-colored mesh is a $2F_o - F_c$ "kick" map[39] contoured at 1σ. Protein residues are shown as sticks colored by element, with carbon as blue. Side chains lacking density, or with ambiguous density, are not shown.

dx.doi.org/10.1021/bi201548p | *Biochemistry* 2012, 51, 769−775

forms a hydrogen bond with Tyr 164 across the binding interface. The breaking of the hydrogen bond between His 249 and Tyr 164 when PEP binds to the enzyme may contribute to the substrate-binding interface becoming weaker in response to PEP binding.[15,28] Perhaps the formation of a hydrogen bond across the substrate-binding interface between His 249 and either Tyr 164 or Glu 161 is important for tetramer stability. Therefore, the addition of PEP may cause a perturbation between these residues and in the quaternary structure of the enzyme to weaken the substrate-binding interface.

Figure 4 shows the relative positions of Glu 161 and Arg 162 in the active sites of the substrate-bound, PGA-bound, and apo crystal structures. In the substrate-bound BsPFK structure, the positively charged Arg 162 interacts with the negatively charged phosphate group of Fru-6-P, and in the PGA-bound structure, the negatively charged Glu 161 replaces Arg 162, thereby decreasing the suitability of the active site for Fru-6-P. These structural features were used to rationalize the low affinity for Fru-6-P displayed by the T-state when PGA was bound.[13] However, previous studies suggest that the switching of Glu 161 and Arg 162 in the active site plays an only minor role in PEP inhibition.[29] Because the apo BsPFK structure was presumed to be in the T-state, we had expected Glu 161 to be poised in the active site of the apo crystal structure.[11,12] However, Arg 162 is in the active site of the apo BsPFK crystal structure with the apo positions of both Arg 162 and Glu 161 matching quite well with the substrate-bound positions (Figure 4).

Figure 5 compares the effector binding site of apo BsPFK to the substrate-bound form and the PGA-bound form. Note that

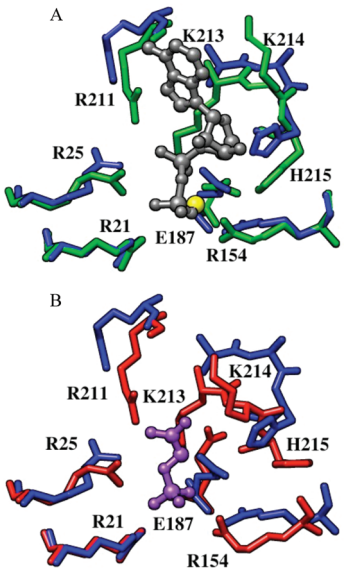

Figure 5. Overlay of residues in the effector binding site of BsPFK. (A) Apo residues colored blue, substrate-bound BsPFK residues colored green, ADP shown as gray balls and sticks, and Mg ion colored yellow. (B) Apo residues colored blue, PGA-bound BsPFK residues colored red, and PGA shown as purple balls and sticks.

the substrate-bound structure has the activator MgADP bound to the effector binding sites as well as the MgATP binding sites. The orientation of residues 213−215 in the apo structure resembles that of the substrate-bound enzyme, except the loop is slightly more open in the apo structure. Arg 211 is not well ordered in the apo structure and can be visualized only in subunit D, where the orientation of Arg 211 is significantly different from those of both of the liganded structures. Arg 211 interacts with the α-phosphate of ADP in the substrate-bound BsPFK. In the PGA-bound BsPFK, Arg 211 interacts with the carboxylate group of PGA. Arg 211 also interacts with the backbone carbonyl oxygen of Ile 320 in both of the liganded structures. However, in the apo BsPFK structure, Arg 211 is positioned so that it interacts only with a water molecule. Therefore, Arg 211 no longer binds with the backbone oxygen of Ile 320. The position of Glu 187 also shows significant deviation relative to both substrate-bound and PGA-bound enzymes. In the substrate-bound structure, the side chain of Glu 187 is coordinated to the magnesium ion of ADP and interacts with Lys 213. In the PGA-bound structure, the side chain of Glu 187 rotates away from the ligand and interacts with Lys 213 and Ser 216. However, in the apo structure, Glu 187 forms a hydrogen bond with a water molecule and no other residue. The significance of Glu 187 was demonstrated by experiments performed with EcPFK in which Glu 187 was changed to an Ala, which alters the allosteric response to PEP in the presence of MgATP.[30,31]

DISCUSSION

When considering the mechanistic basis of allosteric behavior in enzymes, it is important to interpret both the structural and the thermodynamic characteristics of the enzyme simultaneously. The two-state model that has been proposed to explain the allosteric mechanism for BsPFK is based on the differences between the crystal structures of the substrate-bound and PGA-bound enzymes,[13] and this model, as applied to BsPFK, has been found to have a number of deficiencies. The change in position that occurs between Glu 161 and Arg 162 in the active site has been shown not to be responsible for the inhibition by PEP.[29] The principle of reciprocity cannot be understood because few changes are apparent in the vicinity of the allosteric binding site as recognized by Evans and co-workers.[13] Reciprocity acknowledges that whatever affects an allosteric ligand has on the binding of the substrate the same effect is felt by the allosteric ligand when the substrate binds. Finally, it is not obvious how the structural alteration is consistent with the apparent thermodynamic property that entropy rather than enthalpy establishes the sign of the allosteric coupling free energy and hence the nature and magnitude of the allosteric effect.[32]

The key to connecting structural perturbations to the allosteric functional properties of an enzyme can be found by examining more closely the coupling free energy. The coupling free energy between an effector (X) and a substrate (A) quantifies both the nature and the magnitude of a K-type allosteric effect through its sign and absolute value, respectively. The coupling free energy (ΔG_{ax}) is determined using the following equation:

$$\Delta G_{ax} = - RT \ln Q_{ax} \quad (1)$$

where Q_{ax} is the coupling constant that is given by

$$Q_{ax} = \frac{K_{ia}^{\circ}}{K_{ia}^{\infty}} = \frac{K_{ix}^{\circ}}{K_{ix}^{\infty}} \quad (2)$$

where K_{ia}° and K_{ia}^{∞} are the dissociation constants for A in the absence and saturating presence of X, respectively, and K_{ix}° and K_{ix}^{∞} are the dissociation constants for X in the absence and saturating presence of A, respectively.[33,34] Therefore, if ΔG_{ax} is

dx.doi.org/10.1021/bi201548p | *Biochemistry* 2012, 51, 769−775

negative (or $Q_{ax} > 1$), then the allosteric effector is an activator, and if ΔG_{ax} is positive (or $Q_{ax} < 1$), the allosteric effector is an inhibitor. When ΔG_{ax} is equal to zero (or $Q_{ax} = 1$), there is no allosteric effect. These definitions reveal that Q_{ax} is the equilibrium constant for the following disproportionation equilibrium:

$$XE + EA \overset{Q_{ax}}{\longleftrightarrow} XEA + E \quad (3)$$

where E is the apo enzyme, EA is the enzyme bound to the substrate, XE is the enzyme bound to the effector, and XEA is the ternary complex formed when both substrate and effector are bound. This equilibrium depicts the different forms that BsPFK can assume in the presence of a substrate and an allosteric effector. To understand the basis for a K-type allosteric effect, one must understand the poise of this equilibrium. Most importantly, all four enzyme species are involved in determining the value of Q_{ax}. The two-state model is based exclusively on a consideration of the XE and EA forms that describes only the left side of the disproportionation equilibrium and ignores the entire right side and, therefore, does not adequately describe the coupling free energy of the reaction.

The four species of enzyme that contribute to the allosteric mechanism have individual free energies of formation. In other words, the coupling free energy can be defined by subtracting the free energy of formation of EA and XE from that of XEA and E:[35]

$$\Delta G_{ax} = G_{XEA} + G_E - (G_{EA} + G_{XE}) \quad (4)$$

This equation can be converted to the following equivalent expression:

$$\Delta G_{ax} = G_{XEA} - G_E - (G_{EA} - G_E + G_{XE} - G_E) \quad (5)$$

Further simplification of eq 5 can be achieved by denoting each successive pairwise difference with a δ such that

$$\Delta G_{ax} = \delta G_{XEA} - (\delta G_{EA} + \delta G_{XE}) \quad (6)$$

This formulation emphasizes the fact that K-type allosteric effects, which require ΔG_{ax} to be non-zero by definition, arise when the sum of the perturbations in the energetics introduced by the binding of the substrate and allosteric ligand individually is different from the perturbation realized by the binding of both ligands simultaneously. In other words, allosterism arises from a failure of the enzyme to accommodate the energetic perturbations introduced by the binding of each ligand individually when both ligands bind simultaneously. The challenge to the structural biologist is to identify the basis for this failure. Equation 6 emphasizes the central role the apo structure plays in this effort. Each term on the right-hand side of eq 6 utilizes the apo enzyme as an energetic reference state.

Strictly using a structurally based model to describe an allosteric mechanism tends to oversimplify the regulation of the enzyme. However, reconciling the structures of BsPFK with the experimentally measured thermodynamic parameters of the enzyme will lead to understanding the structure−function relationship of the allosteric mechanism. With the addition of the apo BsPFK structure, there are now more relevant structures for the allosteric regulation of BsPFK than for any other PFK enzyme. More importantly, the apo BsPFK structure serves as a necessary reference structure for comparison to the liganded structures. We note that one must focus on the energetics associated with these structures, and not just the structures per se, when making these comparisons.

AUTHOR INFORMATION

Corresponding Author

*Phone: (979) 862-2263. Fax: (979) 845-4295. E-mail: gdr@tamu.edu.

Funding

This work was supported by National Institutes of Health Grant GM033216 and Robert A. Welch Foundation Grants A1543 to GDR and A0015 to JCS.

ABBREVIATIONS

PFK, phosphofructokinase; Fru-6-P, fructose 6-phosphate; F1,6BP, fructose 1,6-bisphosphate; EcPFK, phosphofructokinase I from *E. coli*; BsPFK, phosphofructokinase from *B. stearothermophilus*; PEP, phosphoenolpyruvate; LbPFK, phosphofructokinase from *L. delbrueckii*; PGA, phosphoglycolate; MOPS, 3-(*N*-morpholino)propanesulfonic acid; DTT, dithiothreitol; EPPS, *N*-(2-hydroxyethyl)piperazine-*N*′-3-propanesulfonic acid; rmsd, root-mean-square deviation.

REFERENCES

(1) Krauss, G. (2001) *Biochemistry of signal transduction and regulation*, 2nd ed., Wiley-VCH, Weinheim, Germany.

(2) Voet, D., Voet, J. G., and Pratt, C. W. (2008) *Fundamentals of biochemistry: Life at the molecular level*, 3rd ed., John Wiley & Sons, Hoboken, NJ.

(3) Kemp, R. G., and Foe, L. G. (1983) Allosteric regulatory properties of muscle phosphofructokinase. *Mol. Cell. Biochem. 57*, 147−154.

(4) Byrnes, M., Zhu, X., Younathan, E. S., and Chang, S. H. (1994) Kinetic characteristics of phosphofructokinase from *Bacillus stearothermophilus*: MgATP nonallosterically inhibits the enzyme. *Biochemistry 33*, 3424−3431.

(5) Blangy, D., Buc, H., and Monod, J. (1968) Kinetics of the allosteric interactions of phosphofructokinase from *Escherichia coli*. *J. Mol. Biol. 31*, 13−35.

(6) Blangy, D. (1968) Phosphofructokinase from *E. coli*: Evidence for a tetrameric structure of the enzyme. *FEBS Lett. 2*, 109−111.

(7) Le Bras, G., Deville-Bonne, D., and Garel, J. R. (1991) Purification and properties of the phosphofructokinase from *Lactobacillus bulgaricus*. A non-allosteric analog of the enzyme from *Escherichia coli*. *Eur. J. Biochem. 198*, 683−687.

(8) Paricharttanakul, N. M., Ye, S., Menefee, A. L., Javid-Majd, F., Sacchettini, J. C., and Reinhart, G. D. (2005) Kinetic and structural characterization of phosphofructokinase from *Lactobacillus bulgaricus*. *Biochemistry 44*, 15280−15286.

(9) Rypniewski, W. R., and Evans, P. R. (1989) Crystal structure of unliganded phosphofructokinase from *Escherichia coli*. *J. Mol. Biol. 207*, 805−821.

(10) Shirakihara, Y., and Evans, P. R. (1988) Crystal structure of the complex of phosphofructokinase from *Escherichia coli* with its reaction products. *J. Mol. Biol. 204*, 973−994.

(11) Evans, P. R., and Hudson, P. J. (1979) Structure and control of phosphofructokinase from *Bacillus stearothermophilus*. *Nature 279*, 500−504.

(12) Evans, P. R., Farrants, G. W., and Hudson, P. J. (1981) Phosphofructokinase: Structure and control. *Philos. Trans. R. Soc. London, Ser. B 293*, 53−62.

(13) Schirmer, T., and Evans, P. R. (1990) Structural basis of the allosteric behaviour of phosphofructokinase. *Nature 343*, 140−145.

(14) Tlapak-Simmons, V. L., and Reinhart, G. D. (1994) Comparison of the inhibition by phospho(enol)pyruvate and phosphoglycolate of

phosphofructokinase from *B. stearothermophilus*. *Arch. Biochem. Biophys. 308*, 226−230.
(15) Riley-Lovingshimer, M. R., Ronning, D. R., Sacchettini, J. C., and Reinhart, G. D. (2002) Reversible ligand-induced dissociation of a tryptophan-shift mutant of phosphofructokinase from *Bacillus stearothermophilus*. *Biochemistry 41*, 12967−12974.
(16) Monod, J., Wyman, J., and Changeux, J. P. (1965) On the Nature of Allosteric Transitions: A Plausible Model. *J. Mol. Biol. 12*, 88−118.
(17) French, B. A., Valdez, B. C., Younathan, E. S., and Chang, S. H. (1987) High-level expression of *Bacillus stearothermophilus* 6-phosphofructo-1-kinase in *Escherichia coli*. *Gene 59*, 279−283.
(18) Lovingshimer, M. R., Siegele, D., and Reinhart, G. D. (2006) Construction of an inducible, pfkA and pfkB deficient strain of *Escherichia coli* for the expression and purification of phosphofructokinase from bacterial sources. *Protein Expression Purif. 46*, 475−482.
(19) Valdez, B. C., French, B. A., Younathan, E. S., and Chang, S. H. (1989) Site-directed mutagenesis in *Bacillus stearothermophilus* fructose-6-phosphate 1-kinase. Mutation at the substrate-binding site affects allosteric behavior. *J. Biol. Chem. 264*, 131−135.
(20) Riley-Lovingshimer, M. R., and Reinhart, G. D. (2001) Equilibrium binding studies of a tryptophan-shifted mutant of phosphofructokinase from *Bacillus stearothermophilus*. *Biochemistry 40*, 3002−3008.
(21) Thaller, C., Weaver, L. H., Eichele, G., Wilson, E., Karlsson, R., and Jansonius, J. N. (1981) Repeated seeding technique for growing large single crystals of proteins. *J. Mol. Biol. 147*, 465−469.
(22) Otwinowski, Z., and Minor, W. (1997) Processing of X-ray diffraction data collected in oscillation mode. *Methods Enzymol. 276*, 307−326.
(23) McCoy, A. J. (2007) Solving structures of protein complexes by molecular replacement with Phaser. *Acta Crystallogr. D63*, 32−41.
(24) Adams, P. D., Grosse-Kunstleve, R. W., Hung, L. W., Ioerger, T. R., McCoy, A. J., Moriarty, N. W., Read, R. J., Sacchettini, J. C., Sauter, N. K., and Terwilliger, T. C. (2002) PHENIX: Building new software for automated crystallographic structure determination. *Acta Crystallogr. D58*, 1948−1954.
(25) Emsley, P., and Cowtan, K. (2004) Coot: Model-building tools for molecular graphics. *Acta Crystallogr. D60*, 2126−2132.
(26) Davis, I. W., Leaver-Fay, A., Chen, V. B., Block, J. N., Kapral, G. J., Wang, X., Murray, L. W., Arendall, W. B. III, Snoeyink, J., Richardson, J. S., and Richardson, D. C. (2007) MolProbity: All-atom contacts and structure validation for proteins and nucleic acids. *Nucleic Acids Res. 35*, W375−W383.
(27) Pettersen, E. F., Goddard, T. D., Huang, C. C., Couch, G. S., Greenblatt, D. M., Meng, E. C., and Ferrin, T. E. (2004) UCSF Chimera: A visualization system for exploratory research and analysis. *J. Comput. Chem. 25*, 1605−1612.
(28) Quinlan, R. J., and Reinhart, G. D. (2006) Effects of protein-ligand associations on the subunit interactions of phosphofructokinase from *B. stearothermophilus*. *Biochemistry 45*, 11333−11341.
(29) Kimmel, J. L., and Reinhart, G. D. (2000) Reevaluation of the accepted allosteric mechanism of phosphofructokinase from *Bacillus stearothermophilus*. *Proc. Natl. Acad. Sci. U.S.A. 97*, 3844−3849.
(30) Lau, F. T., and Fersht, A. R. (1987) Conversion of allosteric inhibition to activation in phosphofructokinase by protein engineering. *Nature 326*, 811−812.
(31) Pham, A. S., and Reinhart, G. D. (2001) MgATP-dependent activation by phosphoenolpyruvate of the E187A mutant of *Escherichia coli* phosphofructokinase. *Biochemistry 40*, 4150−4158.
(32) Tlapak-Simmons, V. L., and Reinhart, G. D. (1998) Obfuscation of allosteric structure-function relationships by enthalpy-entropy compensation. *Biophys. J. 75*, 1010−1015.
(33) Weber, G. (1972) Ligand binding and internal equilibria in proteins. *Biochemistry 11*, 864−878.
(34) Weber, G. (1975) Energetics of ligand binding to proteins. *Adv. Protein Chem. 29*, 1−83.
(35) Reinhart, G. D. (2004) Quantitative analysis and interpretation of allosteric behavior. *Methods Enzymol. 380*, 187−203.
(36) Cabrera, R., Baez, M., Pereira, H. M., Caniuguir, A., Garratt, R. C., and Babul, J. (2011) The Crystal Complex of Phosphofructokinase-2 of *Escherichia coli* with Fructose-6-phosphate. *J. Biol. Chem. 286*, 5774−5783.
(37) Banaszak, K., Mechin, I., Obmolova, G., Oldham, M., Chang, S. H., Ruiz, T., Radermacher, M., Kopperschlager, G., and Rypniewski, W. (2011) The Crystal Structures of Eukaryotic Phosphofructokinase from Baker's Yeast and Rabbit Skeletal Muscle. *J. Mol. Biol. 407*, 284−297.
(38) McNicholas, S., Potterton, E., Wilson, K. S., and Noble, M. E. M. (2011) Presenting your structures: The CCP4mg molecular-graphics software. *Acta Crystallogr. D67*, 386−394.
(39) Praaenikar, J., Afonine, P. V., Guncar, G., Adams, P. D., and Turk, D. (2009) Average kick maps: Less noise, more signal...and probably less bias. *Acta Crystallogr. D65*, 921−931.
(40) Luzzati, V. (1952) Traitement statistique des erreurs dans la determination des structures cristallines. *Acta Crystallogr. 5*, 802−810.